EXPERIMENTAL INVESTIGATION OF FLAT PLATE SELF-NOISE REDUCTION USING TRAILING EDGE SERRATIONS

Danielle J. Moreau , Laura A. Brooks , Con J. Doolan
School of Mechanical Engineering, The University of Adelaide,
Adelaide, South Australia, 5005, Australia
danielle.moreau@adelaide.edu.au; laura.brooks@adelaide.edu.au; con.doolan@adelaide.edu.au

Keywords: *Trailing edge noise, flat plate, trailing edge serrations, hot-wire anemometry*

Abstract

This paper presents an experimental study on the noise reduction potential of sawtooth trailing edge serrations at low-to-moderate Reynolds number ($1.6 \times 10^5 < Re_c < 4.2 \times 10^5$, based on chord). The noise radiated by flat plates with both straight and serrated trailing edges has been measured in an anechoic wind tunnel at the University of Adelaide. The trailing edge serrations were found to reduce narrowband noise levels by up to 13 dB. The straight and serrated trailing edge far-field acoustic spectra are scaled according to existing theory and compared to predictions of trailing edge noise obtained using current semi-empirical methods. In addition, velocity spectra measured in the trailing edge near wake region using hot-wire anemometry are related to the far-field noise measurements to give further insight into the serration noise reduction mechanism.

1 Introduction

Airframe noise has been identified as one of the major sources of noise during aircraft approach and landing [1]. As aircraft noise standards become more stringent, airframe noise and in particular airfoil trailing edge noise, will need to be significantly attenuated. Trailing edge noise is also considered to be a significant noise source for fans, wind turbines and underwater vehicles [2, 3]. This type of flow-induced noise is produced by the interaction of turbulent eddies with a sharp trailing edge resulting in the radiation of acoustic energy.

A reduction in trailing edge noise can be achieved by modifying trailing edge geometry so that boundary layer vorticity is scattered into sound with reduced efficiency. Various passive trailing edge modifications such as porous edges [4], brush or comb type extensions [5, 6], shape optimisation [7] and trailing edge serrations have been investigated as a means of reducing trailing edge noise. Trailing edge serrations have been shown both theoretically [8, 9] and experimentally [10]-[16] to significantly attenuate the trailing edge noise radiated into the far-field. The majority of experimental studies on trailing edge serrations have been conducted on full scale wind turbine blades or wind tunnel scale airfoil models at high Reynolds numbers ($Re_c > 5 \times 10^5$, based on chord) [10, 12, 14, 15]. These studies have reported that trailing edge serrations reduce broadband noise levels by up to 7 dB at low frequencies and produce a high frequency noise increase of ~ 2 dB.

The physical mechanisms by which trailing edge serrations reduce trailing edge noise are not yet fully understood. In addition, design rules and empirical scaling laws for trailing edge serrations that relate their noise signatures to Reynolds number and boundary-layer flow properties still need to be derived from experimental data if trailing edge serrations are to be used in practice.

This paper focuses on the noise reduction potential of trailing edge serrations applied to a flat plate at low-to-moderate Reynolds number ($1.6 \times 10^5 < Re_c < 4.2 \times 10^5$). This experimental study has relevance to applications employing small sized airfoils such as small scale wind turbines, unmanned air vehicles (UAVs) and computer and automotive fans, all of which operate at lower Reynolds numbers. The aim of this study is (1) to evaluate acoustic scaling laws for trailing edge serrations to clarify the relationship between noise and Reynolds number and trailing edge flow properties, and (2) to investigate how serrations affect noise production at the trailing edge.

2 Experimental method

2.1 Anechoic wind tunnel facility

Experiments were performed in the anechoic wind tunnel at the University of Adelaide. The anechoic wind tunnel test chamber is 1.4 m × 1.4 m × 1.6 m (internal dimensions) and has walls that are acoustically treated with foam wedges providing a near reflection free environment above 250 Hz. The facility contains a contraction outlet that is rectangular in cross-section with dimensions of 75 mm x 275 mm. The maximum flow velocity of the free jet is ~ 40 m/s and the free-stream turbulence intensity at the contraction outlet is 0.33% [17].

2.2 Test model

The flat plate model used in this study is composed of a main steel body and a detachable trailing edge plate made from brushed aluminum, as shown in Fig. 1 (a). The main body has a span of 450 mm and a thickness of 5 mm. The leading edge (LE) of the main body is elliptical with a semi-major axis of 8 mm and a semi-minor axis of 2.5 mm while the trailing edge (TE) is asymmetrically bevelled at an angle of 12°. Three 0.5 mm thick trailing edge plates were used (one at a time) as shown in Fig. 2 (a): one with a straight, unserrated configuration and two with serrations. The flat plate model with the straight unserrated trailing edge is used as the reference configuration for all tests and so will be referred to as the reference plate hereafter. Two different serration geometries are compared in this study, both with root-to-tip amplitude of $2h = 30$ mm: one with a wavelength of $\lambda = 3$ mm ($\lambda/h = 0.2$, termed narrow serrations) and the other with $\lambda = 9$ mm ($\lambda/h = 0.6$, termed wide serrations). The two geometrical parameters h and λ are defined in Fig. 1 (b). As shown in Fig. 2 (b), the root of the serrations is aligned with the trailing edge of the main body so that only the serrated component of the trailing edge plate is exposed to the flow. The area of the reference plate is equivalent to that of the flat plate with serrated trailing edges giving the same effective wetted surface area in all three test cases. The serrated and reference plate models all have a mean chord of 165 mm.

The trailing edge plate is fastened to the main body with 24 M2 × 0.4 screws. These screws protruded slightly (< 0.4 mm) into the flow below the lower flat surface of the plate model; however, this was consistent for all three plate configurations. Hot-wire measurements within the boundary layer on the lower flat surface of the plate downstream of the screws confirmed that any flow disturbances created at the screws dissipated well before the trailing edge. The method of trailing edge attachment used in this study avoids bluntness at the root of the serrations that may produce vortex shedding and a tonal noise component. The flat plate model was held between two side plates and attached to the contraction at zero angle of attack as shown in Fig. 2 (b). The span of the flat plate models extends beyond the width of the contraction outlet (see Fig. 2 (b)) to eliminate the noise produced by the interaction of the side plate boundary layers with the model leading edge.

2.3 Acoustic and velocity measurements

Acoustic measurements were recorded at a single observer location using a B&K 1/2" microphone (Model No. 4190) located 554 mm di-

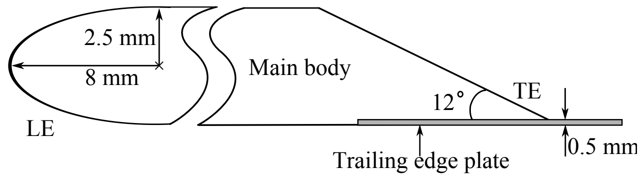

(a) The flat plate model.

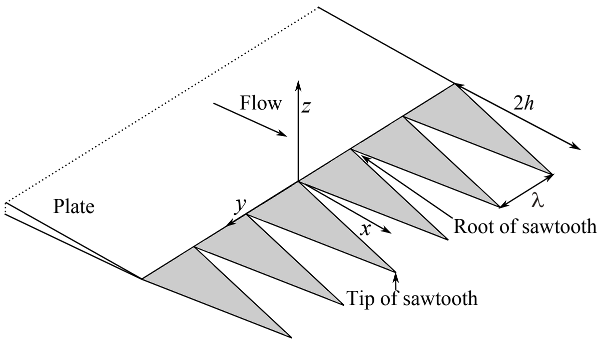

(b) Sawtooth serrations at the trailing edge of a flat plate with root-to-tip amplitude of $2h$ and wavelength of λ.

Fig. 1 : Schematic diagram of the flat plate model with trailing edge serrations.

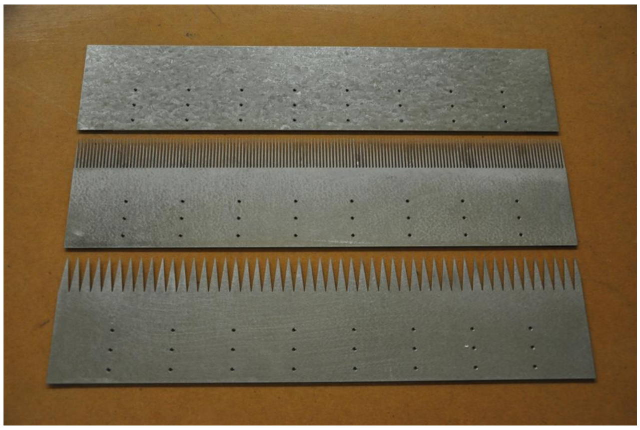

(a) Trailing edge plates. Top: straight unserrated trailing edge (reference), middle: narrow serrations with $\lambda = 3$ mm, bottom: wide serrations with $\lambda = 9$ mm.

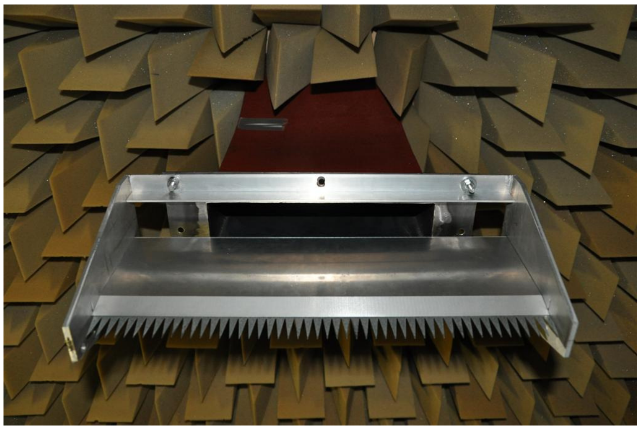

(b) The flat plate model with wide trailing edge serrations held between the side plates and attached to the contraction outlet.

Fig. 2 : The trailing edge plates and the flat plate model in situ.

rectly below the trailing edge of the reference plate. Hot-wire anemometry was used to obtain unsteady velocity data in the wake of the serrated and reference plate models. A TSI 1210-T1.5 single wire probe with wire length of $L = 1.27$ mm and a wire diameter of $d = 3.81$ μm was used in experiments. The sensor was connected to a TSI IFA300 constant temperature anemometer system and positioned using a Dantec automatic traverse with 6.25 μm positional accuracy. The traverse allowed continuous movement in the streamwise (x), spanwise (y) and vertical (z) directions. The co-ordinate system used in this study is shown in Fig. 1 (b). The origin of the co-ordinate system is located at centre span at the root of the trailing edge serrations.

Experiments were conducted at free-stream velocities between $U_\infty = 15$ and 38 m/s corresponding to Reynolds numbers, $Re_c = 1.6 \times 10^5$ and 4.2×10^5, respectively. Acoustic and flow data were recorded for each flat plate model using a National Instruments board at a sampling frequency of 5×10^4 Hz for a sample time of 8 s.

3 Experimental results

3.1 Acoustic measurements for the reference plate with straight trailing edge

Before investigating the noise reduction effects of trailing edge serrations in Section 3.2, the noise produced by the reference plate with straight trailing edge is examined in this section.

Figure 3 shows the far-field acoustic spectra for the reference plate with a straight trailing edge at free-stream velocities between $U_\infty = 15$ and 38 m/s. The spectra in this figure follow a clear trend with broadband noise levels decreasing with a reduction in flow velocity. This is particularly evident at lower frequencies (< 1 kHz) where higher noise levels are measured. In addition, a broad peak is observed in the noise spectra at high frequencies (e.g. at 8.5 kHz for $U_\infty = 38$ m/s). This peak reduces in frequency and amplitude with decreasing flow speed and is attributed to vortex shedding from the trailing edge.

According to Blake [2], narrowband blunt trailing edge vortex shedding noise is negligible if the trailing edge is sufficiently sharp such that bluntness parameter $h/\delta^* < 0.3$ where h is the thickness of the trailing edge and δ^* is the boundary layer displacement thickness. While the boundary layer properties have not been directly measured in this study, they can be approximated using the expressions for a turbulent boundary layer at zero pressure gradient on a flat plate as follows [18]

$$\delta = 8\delta^*, \text{ and} \tag{1}$$

$$\frac{\delta}{c} = \frac{0.37}{Re_c^{1/5}}, \tag{2}$$

where δ is the boundary layer thickness and c is the plate chord. The boundary layer properties for the reference plate at flow speeds between $U_\infty = 15$ and 38 m/s calculated using Eqns. (1) and (2) are given in Table 1. As shown in this table, the bluntness parameter h/δ^* is well above 0.3 for all free-stream velocities between $U_\infty =$ 15 and 38 m/s indicating that narrowband noise contributions due to blunt trailing edge vortex shedding can be expected.

For an idealized (non-compact) semi-infinite flat plate of zero thickness, the amplitude of the radiated trailing edge noise scales proportionally with M^5, where M is the free-stream Mach number [19]. The one-third-octave band spectra for the reference plate at flow speeds between $U_\infty =$ 15 and 38 m/s are normalised by M^5 in Fig. 4:

$$Lp_{1/3}\,\text{scaled1} = Lp_{1/3} - 50\log_{10}(M), \tag{3}$$

where $Lp_{1/3}$ is the far-field acoustic spectra in one-third-octave bands. The frequency of trailing edge noise is expected to scale according to $f \sim U_\infty/l$, where l is the characteristic length scale. In Fig. 4, trailing edge thickness, h, is used as the characteristic length scale and the normalised one-third-octave band spectra for the reference plate are plotted against Strouhal number based on trailing edge thickness, $St_h = fh/U_\infty$.

Figure 4 shows that an M^5 power law gives a good collapse of the reference plate noise spectra between $U_\infty = 15$ and 38 m/s. Spectral data that are originally spread by almost 40 dB are collapsed to within 7 dB. The one-third-octave band noise levels of the reference plate therefore increase according to an M^5 power law.

Figure 4 shows that at flow speeds between

Table 1: Flat plate boundary layer properties between $U_\infty = 15$ and 38 m/s.

U_∞, m/s	δ, mm	δ^*, mm	$h/\delta*$
38	4.7	0.53	0.84
35	4.8	0.60	0.82
30	5.0	0.62	0.80
25	5.2	0.64	0.77
20	5.4	0.67	0.74
15	5.7	0.71	0.70

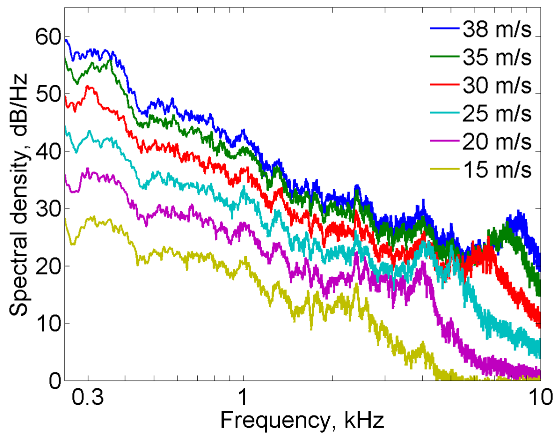

Fig. 3 : Far-field acoustic spectra for the reference plate at $U_\infty = 15$ - 38 m/s.

$U_\infty = 15$ and 38 m/s, vortex shedding noise contributions occur at a Strouhal number of $St_h = 0.08 - 0.11$. This is in good agreement with several other studies on flat plate trailing edge noise [20, 21, 5].

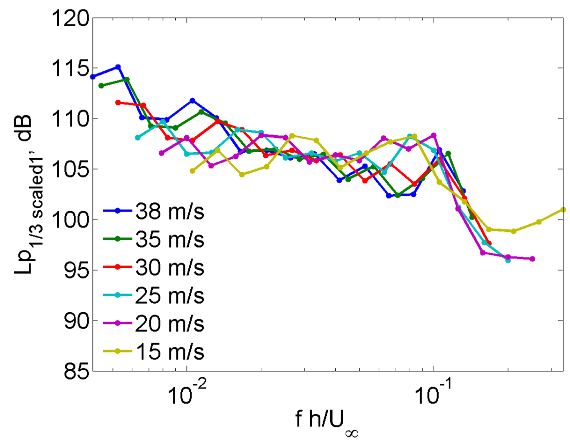

Fig. 4 : Normalised one-third octave band acoustic spectra for the reference plate scaled with M^5 with h as the characteristic length scale at $U_\infty = 15$ - 38 m/s.

Boundary layer displacement thickness, δ^*, is commonly considered the most relevant scaling parameter for trailing edge noise [20]. The one-third-octave band spectra for the reference plate at flow speeds between $U_\infty = 15$ and 38 m/s are normalized by both M^5 and δ^* in Fig. 5 (a):

$$Lp_{1/3}\ \mathrm{scaled2} = Lp_{1/3} - 50\log_{10}(M) - 10\log_{10}(\delta^*), \tag{4}$$

and δ^* is used as the characteristic length scale. The spectra in Fig. 5 (a) coalesce to within 6 dB and the vortex shedding noise peak occurs at $St^*_\delta \approx 0.13$ for all flow speeds between $U_\infty =$ 15 and 38 m/s. This excellent scaling with the parameter δ^* is expected given that the source of trailing edge noise is the turbulent flow field about the trailing edge and δ^* is a property of the flow field within the source area.

The BPM model developed by Brooks et al. [21] is a commonly used semi-empirical prediction method for estimating airfoil self-noise. The BPM model was derived from existing theory and aeroacoustic data for NACA0012 airfoil models at a wide range of Reynolds numbers. The

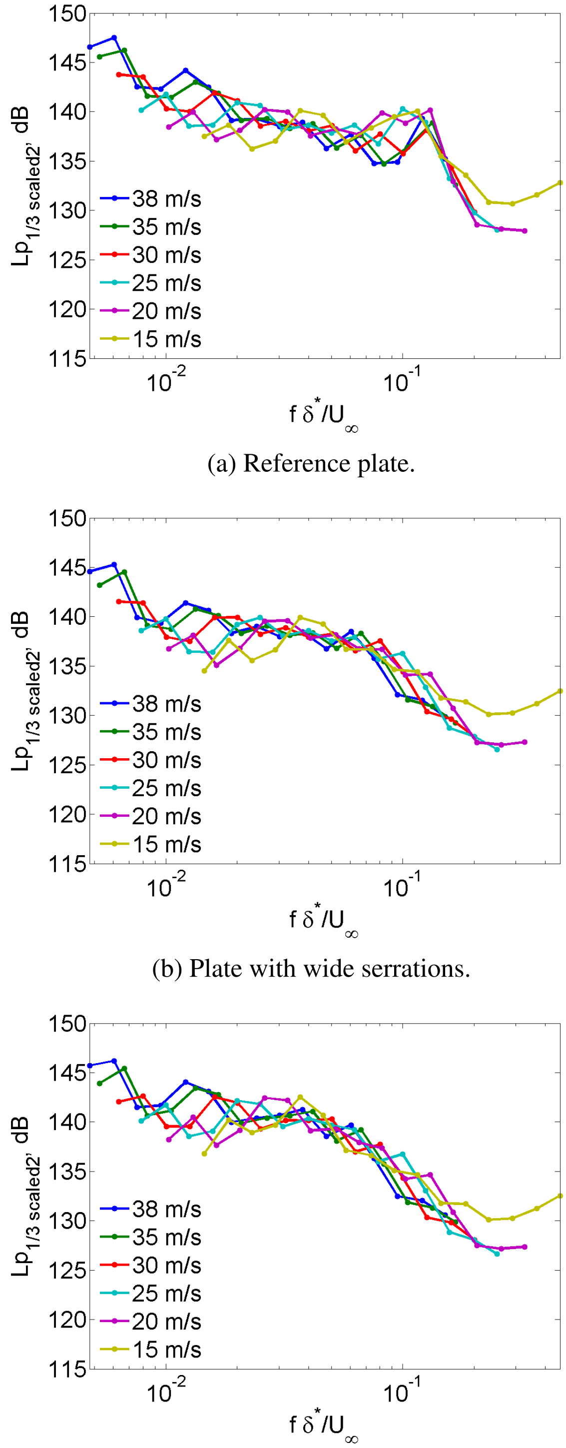

(a) Reference plate.

(b) Plate with wide serrations.

(c) Plate with narrow serrations.

Fig. 5 : Normalised one-third octave band acoustic spectra for the reference plate and the plate with trailing edge serrations scaled with M^5 and δ^* with δ^* as the characteristic length scale at $U_\infty = 15$ - 38 m/s.

one-third-octave band spectra for the reference plate are compared to the noise spectra predicted with the BPM model in Fig. 6 (a). In this figure, boundary layer displacement thickness, δ^*, is used as the characteristic length scale and the noise spectra predicted with the BPM model have been calculated using NAFNoise [22] (NREL AirFoil Noise) at equivalent conditions to those used in experiments here. While there are significant differences in the spectral shape and level at low frequencies ($St_{d^*} < 0.05$), the BPM model is in fairly good agreement with experimental data when $St_{d^*} > 0.05$. Poor predictions at low frequencies can be attributed to the fact that the BPM model was derived from experimental data that was at times truncated at low and high frequencies. This truncation was done to eliminate the influence of extraneous noise sources that were expected to significantly affect the noise levels in the low and high frequency regions. Examining the results of Brooks et al. [21] shows that experimental data used in the derivation of the BPM model at zero angle of attack is well predicted at high Reynolds numbers but underpredicted in the low frequency region at low Reynolds numbers. It is also worth noting that the low frequency experimental data in this study has been analysed differently to that used in development of the BPM model so differences are expected between the model and experimental data at low frequencies.

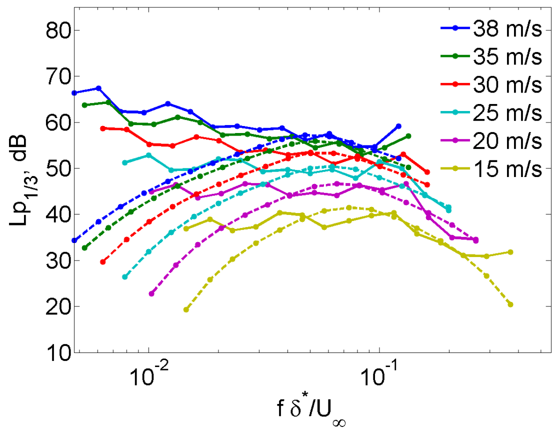

(a) Reference plate.

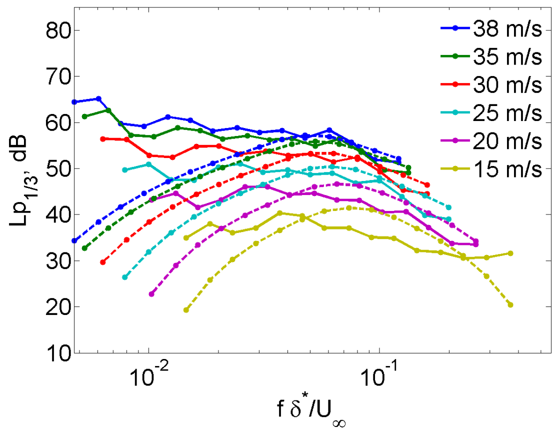

(b) Wider serrations

Fig. 6 : One-third octave band acoustic spectra for the reference plate and the plate with wide serrations compared to the BPM model with δ^* as the characteristic length scale at $U_\infty = 15$ - 38 m/s.

3.2 Acoustic measurements for the plate with trailing edge serrations

Figure 7 shows the narrowband far-field acoustic spectra for the reference plate and the two plates with trailing edge serrations at free-stream velocities of $U_\infty = 15$ and 38 m/s. The background noise spectra are also shown in this figure for comparison. Figure 7 clearly shows that both serration geometries are effective in reducing the high frequency trailing edge vortex shedding noise component. Reductions of up to 13 dB are achieved at frequencies where trailing edge vortex shedding noise is dominant (e.g. at 8.5 kHz for $U_\infty = 38$ m/s).

Figure 8 shows the attenuation achieved with the trailing edge serrations at flow speeds between $U_\infty = 15$ and 38 m/s in one-third-octave bands. In this figure, boundary layer displacement thickness, δ^*, is used as the characteristic length scale. Figure 8 shows that the attenuation achieved with trailing edge serrations collapses to within 3 dB over a wide range of frequencies when the characteristic length scale is δ^*. Both trailing edge serration geometries are observed to achieve a significant reduction in vortex shedding noise contributions at $St^*_\delta \approx 0.13$ and a minor noise reduction in the low frequency broad-

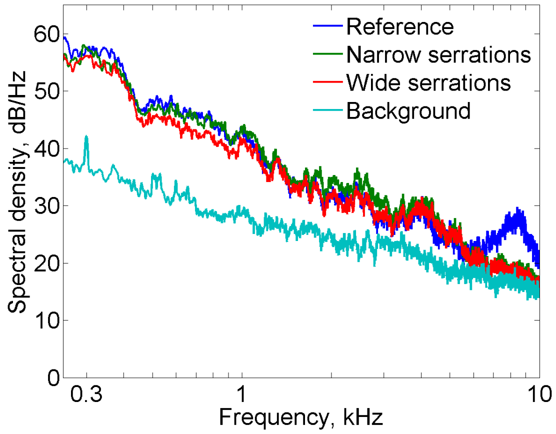

(a) $U_\infty = 38$ m/s.

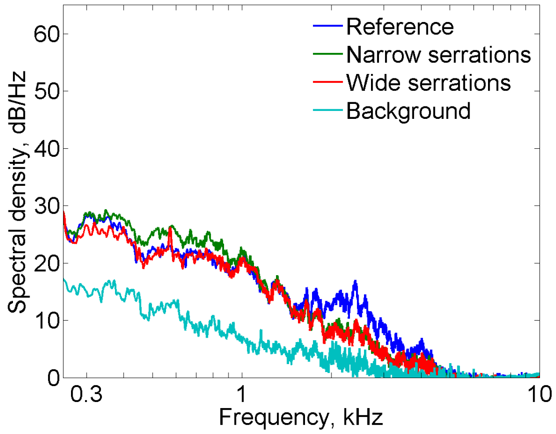

(b) $U_\infty = 15$ m/s.

Fig. 7 : Far-field acoustic spectra for the reference plate and the plate with trailing edge serrations compared to background noise levels.

band noise. The wide serrations attenuate broadband noise levels by up to 3 dB at low frequencies ($St^*_\delta < 0.03$) and significantly attenuate the trailing edge vortex shedding noise component (at $St^*_\delta \approx 0.13$) by up to 8 dB. Narrow serrations slightly reduce broadband noise levels by up to 2 dB at low frequencies ($St^*_\delta < 0.015$) and produce a significant noise reduction of up to 8 dB in the trailing edge vortex shedding noise component (at $St^*_\delta \approx 0.13$). Unlike wide serrations, the narrow ones have an adverse effect on the noise in the mid frequency region, producing a noise increase of up to 3 dB at $0.015 < St^*_\delta < 0.08$.

Figure 8 shows that flow velocity has a measurable effect on the noise reduction potential of trailing edge serrations. The maximum noise reduction is achieved at higher flow speeds with the attenuation level gradually reducing with a decrease in flow speed. Comparing Figs. 8 (a) and (b) shows that the wide serrations clearly outperform the narrow ones by achieving higher levels of low frequency attenuation over a larger frequency range and no noise increase in the mid frequency region.

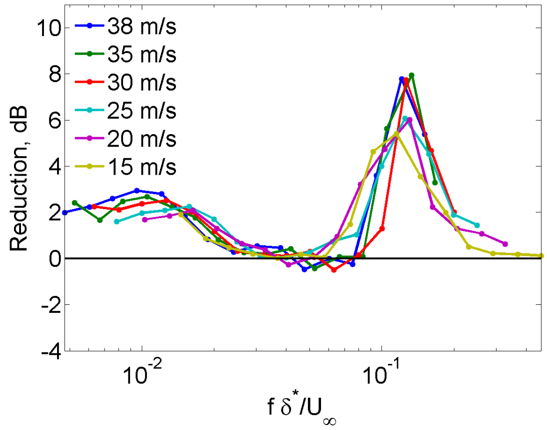

(a) Wide serrations.

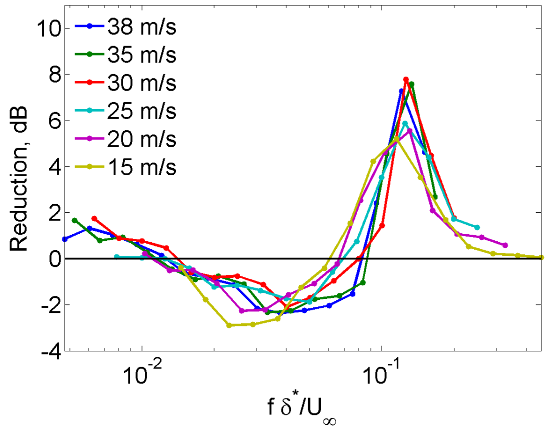

(b) Narrow serrations.

Fig. 8 : One-third octave band attenuation achieved with the trailing edge serrations with δ^* as the characteristic length scale at $U_\infty = 15$ - 38 m/s.

The one-third-octave band acoustic spectra for the flat plate with trailing edge serrations at flow speeds between $U_\infty = 15$ and 38 m/s are normalized by M^5 and δ^* in Figs. 5 (b) and (c). In this figure, the one-third-octave band spectra have been normalized according to Eq. (4) and δ^* is used as the characteristic length scale. For both serration geometries, the spectra are observed to collapse within 6 dB. The far-field noise produced by the serrated trailing edges therefore increases with M^5 in accordance with trailing edge theory and scales in the same way as the noise radiated by the straight trailing edge.

The one-third-octave band spectra for the flat plate with wide serrations are compared to the noise spectra predicted with the BPM model [21] in Fig. 6 (b). This figure shows that again the BPM model significantly underpredicts noise levels in the low frequency region ($St_{d^*} < 0.05$). At high frequencies ($St_{d^*} > 0.05$) however, where the greatest noise reductions are measured, the BPM model overpredicts the noise produced by the serrated trailing edge and this becomes more evident as the flow speed is reduced. A similar result is observed when the spectra for the flat plate with narrow serrations are compared with the BPM model.

3.3 Wake velocity spectra

As the turbulent flow field about the trailing edge is the source of trailing edge noise, velocity spectra measured in the very near wake of the straight and serrated trailing edges are examined in this section to gain insight into the serration noise reduction mechanism.

Figure 9 shows the narrowband velocity spectra measured at centre span in the near wake of the flat plate model with straight and serrated trailing edge at free-stream velocities of $U_\infty = 15$ and 38 m/s. In this figure, the reference plate spectra have been measured at $x/c = 0.1$, $z/c = 0$ which corresponds to a position 1 mm downstream of the straight trailing edge. The serrated trailing edge spectra have been measured at $x/c = 0.19$, $z/c = 0$ which corresponds to a position 1 mm downstream of the serrated trailing edge and ‘tip’ refers to position downstream of the tip of a single serrated tooth while ‘valley’ refers to a position in the space mid-way between two serrated teeth.

The velocity spectra at $U_\infty = 38$ m/s in Fig. 9 (a) all show high energy at frequencies below 500 Hz, consistent with the high levels of low frequency trailing edge noise in Fig. 7 (a). This low frequency energy is likely due to eddies or convected perturbations in the flow. High energy velocity fluctuations are not observed at low frequencies in the velocity spectra at $U_\infty = 15$ m/s (see Fig. 9 (b)). Similarly, the acoustic far-field spectra do not display an excess in energy below 500 Hz (see Fig. 7 (b)).

At both $U_\infty = 15$ and 38 m/s, the velocity spectra for the reference plate in Fig. 9 show a broad high frequency peak at the same frequencies as the peak in the reference plate noise spectra (see Fig. 7). This supports the theory that vortex shedding at the trailing edge is the source of the broad high frequency peak in the reference plate noise spectra. No high frequency peak is observed in the spectra for the serrated trailing edges. This agrees with the noise spectra in Fig. 7 which show that serrations attenuate the vortex shedding noise component. Trailing edge serrations therefore reduce trailing edge vortex shedding noise by suppressing vortex shedding from the trailing edge. This indicates that trailing edge serrations reduce this trailing edge noise component by changing the behaviour of the hydrodynamic field at the source location.

4 Conclusion

This paper has presented results of an experimental investigation on the noise produced by trailing edge serrations. Trailing edge serrations were found to minimise broadband noise levels at low frequencies by up to 3 dB and achieve significant attenuation of up to 13 dB in blunt vortex shedding noise contributions at high frequencies. The noise levels produced by both the straight and serrated trailing edge increase with M^5 in accordance with trailing edge theory. In addition, the noise spectra for both the straight and serrated trailing edge were found to scale well with trailing edge boundary layer displacement thickness.

Experimental results presented in this paper suggest that the noise reduction capability of trailing edge serrations is related to their influ-

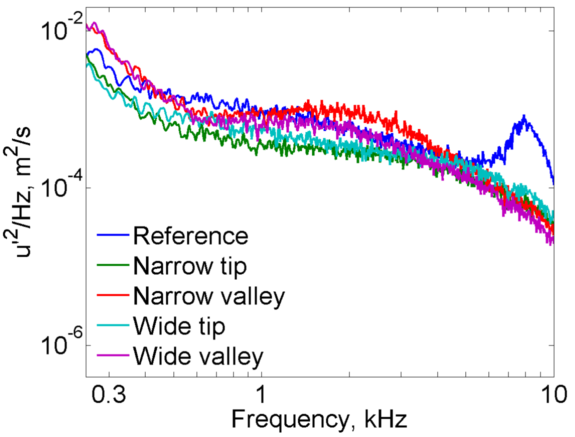

(a) $U_\infty = 38$ m/s.

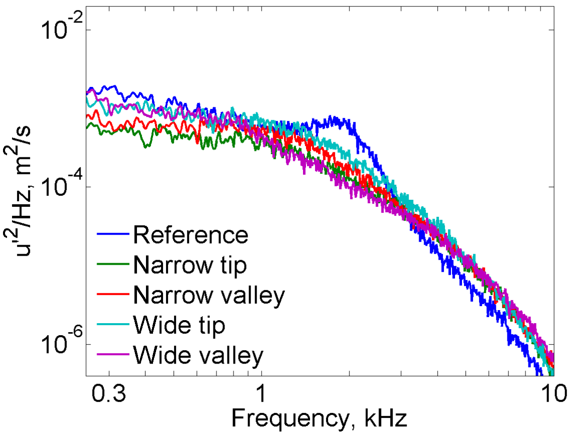

(b) $U_\infty = 15$ m/s.

Fig. 9 : Trailing edge velocity spectra for the reference plate and the plate with trailing edge serrations.

ence on the hydrodynamic field at the source location. To verify this hypothesis, a more comprehensive acoustic and flow dataset is required.

5 Acknowledgment

This work has been supported by the Australian Research Council under grant DP 1094015 “The mechanics of quiet airfoils”.

References

[1] D.P. Lockard and G.M. Lilley. *The airframe noise reduction challenge.* Technical Report NASA/TM-2004-213013, NASA Langley Research Center, 2004.

[2] W.K. Blake. *Mechanics of Flow Induced Sound and Vibration*, volume II: Complex flow-structure interactions. Academic Press, New York, 1986.

[3] S. Oerlemans, M. Fisher, T. Maeder, and K. Kogler. Reduction of wind turbine noise using optimized airfoils and trailing-edge serrations. *AIAA Journal*, 47(6):1470–1481, 2009.

[4] M. Herr and J. Reichenberger. In search of airworthy trailing-edge noise reduction means. In *17th AIAA/CEAS Aeroacoustics Conference*, Portland, Oregon, 5–8 June 2011.

[5] M. Herr and W. Dobrzynski. Experimental investigations in low-noise trailing-edge design. *AIAA Journal*, 43(6):1167–1175, 2005.

[6] M. Herr. On the design of silent trailing-edges. *New Results in Numerical and Experimental Fluid Mechanics VI*, 96:430–437, 2007.

[7] R.F. Jones, C.J. Doolan and M.D Teubner, Minimization of trailing edge noise by parametric airfoil shape modifications. In *17th AIAA/CEAS Aeroacoustics Conference*, Portland, Oregon, 5–8 June 2011.

[8] M.S. Howe. Aerodynamic noise of a serrated trailing edge. *Journal of Fluids and Structures*, 5:33–45, 1991.

[9] M.S. Howe. Noise produced by a sawtooth trailing edge. *Journal of the Acoustical Society of America*, 90(1):482–487, 1991.

[10] K.A. Braun, N.J.C.M. van der Borg, A.G.M. Dassen, F. Doorenspleet, A. Gordner, J. Ocker, and R. Parchen. Serrated trailing edge noise (STENO). In *European Wind Energy Conference*, Nice, France, 1–5 March 1999.

[11] T. Dassen, R. Parchen, J. Bruggeman, and F. Hagg. Results of a wind tunnel study on the reduction of airfoil self-noise by the application of serrated blade trailing edges. In *European Union Wind Energy Conference and Exhibition*, Gothenburg, Sweden, 20 – 24 May 1996.

[12] R. Parchen, W. Hoffmans, Q. Gordner, K.A. Braun, van der Borg N.J.C.M, and A.G.M Dassen. Reduction of airfoil self-noise at low mach number with a serrated trailing edge. In *Sixth International Congress on Sound and Vibration*, Copenhagen, Denmark, 5– 8 July 1999.

[13] T.P. Chong, P. Joseph, and M. Gruber. An experimental study of airfoil instability noise with

trailing edge serrations. In *16th AIAA/CEAS Aeroacoustics Conference*, Stockholm, Sweden, 7 – 9 June 2010.

[14] M. Gruber, P. F. Joseph, and Chong T. P. Experimental investigation of airfoil self noise and turbulent wake reduction by the use of trailing edge serrations. In *16th AIAA/CEAS Aeroacoustics Conference*, Stockholm, Sweden, 7 – 9 June 2010.

[15] M. Gruber, P. F. Joseph, and T. P Chong. On the mechanisms of serrated airfoil trailing edge noise reduction. In *17th AIAA/CEAS Aeroacoustics Conference*, Portland, Oregon, 5–8 June 2011.

[16] D.J. Moreau, L.A. Brooks and C.J. Doolan. Flat plate self-noise reduction at low-to-moderate Reynolds number with trailing edge serrations. In *Acoustics 2011*, Gold Coast, Australia, 2–4 Nov 2011.

[17] D.J. Moreau, L.A. Brooks and C.J. Doolan. Broadband trailing edge noise from a sharp-edged strut. *J. Acoust. Soc. Am.*, 129(5):2820–2829, 2011.

[18] T. Cebeci and P. Bradshaw. *Momentum Transfer in Boundary Layers*. Hemisphere Publishing Corporation, Washington, 1977.

[19] J.E. Ffowcs Williams and L.H. Hall. Aerodynamic sound generation by turbulent flow in the vicinity of a scattering half plane. *J. Fluid Mech.*, 40:657–670, 1970.

[20] T.F. Brooks and T.H. Hodgson. Prediction and comparison of trailing edge noise using measured surface pressures. In *6th AIAA Aeroacoustics Conference*, Hartford, Conn., 4–6 June 1980.

[21] T.F. Brooks, S. Pope, and M.A Marcolini. Airfoil self-noise and prediction. Technical report, NASA Reference Publication 1218, 1989.

[22] P. Moriaty. NWTC design codes: NAFnoise, 2006. http://wind.nrel.gov/designcodes/simulators/NAFNoise/

[23] M.J. Lighthill. On sound generated aerodynamically: General theory. *Proceedings of the Royal Society of London*, A211:564–587, 1952.

Copyright Statement